

## Control of self-replicating patterns in a model reaction-diffusion system

Nita Parekh, V. Ravi Kumar, and B. D. Kulkarni

Chemical Engineering Division, National Chemical Laboratory, Pune-411 008, India

(Received 26 June 1995)

Spatiotemporal patterns, e.g., spots, which replicate, grow, and die as solutions of nonlinear reaction-diffusion models are interesting because of their striking resemblance to the self-replicating phenomena observed in many important physical, chemical, and biological processes, e.g., micelles, living cells, and DNA. With this viewpoint we considered the characterization of a model self-replicating system from limited and inaccurate system information. We also addressed control goals that are relevant to many natural processes exhibiting this phenomenon, such as altering and arresting the growth of replication.

PACS number(s): 82.20.Wt, 05.40.+j, 87.15.He

Pattern formation in reaction-diffusion systems has been extensively studied both theoretically and experimentally [1]. These systems exhibit a variety of spatiotemporal patterns such as target, striped, or hexagonal patterns and traveling waves [2]. Recent experiments with thin two-dimensional gel laboratory reactors have confirmed that these patterns can arise for nonlinear reaction-diffusion systems uncontaminated by convection effects [3]. Interestingly, a new class of patterns, e.g., spots, which replicate, grow, and die as solutions of mathematical reaction-diffusion models [4,5] has been observed. It is important to note that for a ferrocyanide-iodate-sulphite reaction in the gel reactor [6] similar replicating patterns have now also been observed experimentally. In general, these results seem to further substantiate Turing's belief in the commonality of some of the operating mechanisms in many physical, chemical, and biological systems [7].

The phenomenon of self-replication is observed in many chemical and biological systems, e.g., micelles and reverse micelles [8], morphogenesis of living cells [7], and DNA and RNA oligomers [9]. The underlying mechanism of replication in these systems does seem to indicate the presence of autocatalytic feedback steps, unequal diffusion rates for the interacting species, and a spatial domain defined by boundaries. It is notable that the phenomenological description of the simple nonlinear reaction-diffusion models does include the above characteristic features [4]. These models may therefore be used as prototypes towards building up a sound theoretical basis for understanding the phenomenon of replication in more complex and realistic systems. With this viewpoint, we first attempted to characterize the mathematical model under the constraints of inaccurate knowledge of the system parameters and available dynamical data. We further studied the possibility of controlling the model replicating system with objectives which are general and important for systems exhibiting this phenomenon, viz., arresting the growth of replication; accelerating their rates; altering the system to an earlier stage in its replicating behavior from a comparatively more evolved dynamical state; and activating a dormant system to replicate in a controlled way.

A simple reaction-diffusion model in one spatial dimension, exhibiting the phenomenon of replication is (in dimensionless units) [4]

$$\frac{\partial u(x,t)}{\partial t} = D_u \frac{\partial^2 u(x,t)}{\partial x^2} - u(x,t)v^2(x,t) + A'[1 - u(x,t)], \quad (1)$$

$$\frac{\partial v(x,t)}{\partial t} = D_v \frac{\partial^2 v(x,t)}{\partial x^2} + u(x,t)v^2(x,t) - (A' + B)v(x,t). \quad (2)$$

The underlying reaction mechanism is autocatalytic with two steps, viz.,  $U + 2V \rightarrow 3V$  and  $V \rightarrow P$  with  $P$  an inert product [10]. Here,  $u(x,t)$  and  $v(x,t)$ , respectively, represent the concentrations of the two reactant species with  $D_u$  and  $D_v$  the corresponding diffusion coefficients (with  $D_u > D_v$ ),  $A'$  is a feed parameter, and  $B$  a rate constant for the second step in the reaction mechanism. Figure 1 depicts the typical spatial and temporal distribution of the slowly diffusing species,  $v(x,t)$ , obtained on Euler integration of the above one-dimensional (1D) model for the ratio of the diffusion coefficients  $\delta (= D_v/D_u) = 0.01$  [4]. The simulation was carried out on a 1D lattice of 256 sites, with spatial mesh size  $dx = 0.2$  and time step  $dt = 0.01$ . The entire system was initially placed in a homogeneous stationary state  $u(x,0) = 1$ ,  $v(x,0) = 0$  with a finite perturbation  $u(x,0) = 0.5$ ,  $v(x,0) = 0.25$  given to the system in the central region of the lattice ( $20.8 \leq x \leq 30.6$ ). The dynamic effects of the perturba-

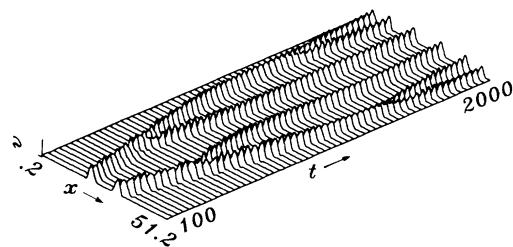


FIG. 1. Self-replicating reaction-diffusion pattern in  $v(x,t)$  ( $A' = 0.03, B = 0.059, D_u = 1.0, D_v = 0.01$ ). ( $v$  axis scale:  $-0.19, 1.59$ .)

tion are shown in Fig. 1 where the peaks that initially develop replicate structurally in time (see Fig. 1) until the entire domain is finally filled with a periodic distribution of similar peaks. For the 1D system, this distribution corresponds to the nonhomogeneous stationary solution of the system equations [4]. A similar behavior was also observed in the dynamics of the other species,  $u(x,t)$  with the difference that regions of high  $v(x,t)$  correspond to regions of low  $u(x,t)$ . For a corresponding 2D system it has been shown that the patterns can become exceedingly complex, especially when the nonhomogeneous stationary solution is unstable [4]. For investigating the behavior of a process exhibiting the phenomenon of replication, we may choose to regard the simulated dynamics illustrated in Fig. 1 as that arising from an experimental system and shall henceforth use the terminology *replicating process* whenever referring to it.

Our first aim was to study the possible dynamical synchronization of the spatially extended replicating process (shown in Fig. 1) with that of a mathematical model for differing initial conditions. In real situations, however, it may not always be possible to monitor the dependent variable signals ( $u(x,t), v(x,t)$ ) over the entire spatial domain. Hence in the synchronization studies described below restrictions in the availability of time-series data have been assumed. For the sake of clarity in presentation let us first distinguish the mathematical model from that used for *simulating* the replicating process. We do so by rewriting the process Eqs. (1) and (2) as

$$\begin{aligned} \partial \hat{u}(x,t) / \partial t = & D_u \partial^2 \hat{u}(x,t) / \partial x^2 - \hat{u}(x,t) \hat{v}^2(x,t) \\ & + \hat{A} [1 - \hat{u}(x,t)] , \end{aligned} \quad (3)$$

$$\begin{aligned} \partial \hat{v}(x,t) / \partial t = & D_v \partial^2 \hat{v}(x,t) / \partial x^2 + \hat{u}(x,t) \hat{v}^2(x,t) \\ & - (\hat{A} + B) \hat{v}(x,t) , \end{aligned} \quad (4)$$

where ( $\hat{u}(x,t), \hat{v}(x,t)$ ) now denote the respective mathematical model variables. Also note that the feed flow parameter  $A'$  in Eqs. (1) and (2) has now been replaced by  $\hat{A}$  in the above model [Eqs. (3) and (4)]. This change in notation allows the specification of an inaccurate parameter value in the mathematical model (i.e., when  $\hat{A} \neq A'$ ). Effectively, the mathematical model dynamics is then described by solving a coupled set of  $2N$  discrete equations in the spatial domain obtained on Euler discretization of Eqs. (3) and (4). Here,  $N$  is the total number of lattice sites employed for discretization at equally spaced intervals  $dx$ . Further, it is assumed that time-series signals from the process are available only from some specified  $n_d$  ( $\ll N$ ) lattice sites in the spatial domain. In practice, the monitored process data at these lattices sites may be corrupted with measurement noise. In simulation studies, therefore, this feature may be incorporated by introducing measurement noise  $\eta(j,t)$  of strength  $\gamma$  and following a Gaussian distribution, viz.,

$$u'(j,t) = [u(j,t) + \gamma \eta(j,t)]$$

and

$$v'(j,t) = [v(j,t) + \gamma \eta(j,t)] ,$$

where  $u'(j,t)$  and  $v'(j,t)$  are the measured process signals. The model equations pertaining to these specified nodes are then governed by

$$\hat{u}(j,t) = u'(j,t) , \quad (5)$$

$$\hat{v}(j,t) = v'(j,t) . \quad (6)$$

In other words, the time-series signals  $u'(j,t)$  and  $v'(j,t)$  from the process at the specified  $n_d$  nodes are dynamically passed on to the mathematical model [11]. On assuming the availability of time-series signals from, say, every 10th lattice site ( $n_d = 25$ ) and using the driving condition given by Eqs. (5) and (6), complete synchronization between the process and model dynamics was observed over the entire spatial domain for arbitrarily chosen initial conditions in the mathematical model [i.e.,  $\hat{u}(i,0) \neq u'(i,0)$  and  $\hat{v}(i,0) \neq v'(i,0)$ ] (results not presented). Synchronization in the dynamics was also possible on a significant reduction in the number of available driving signals,  $n_d$  corresponding only to every maxima position in ( $u', v'$ ) (see Fig. 1) in the nonhomogeneous regions of the dynamically evolving replicating pattern. It is important to note that these studies tacitly assumed that parameter specifications in the model correspond to those of the replicating process (i.e.,  $\hat{A} = A'$ ).

A study for synchronizing the process and model dynamics was undertaken for a realistic situation when the exact value of the process feed flow rate ( $A'$  in Fig. 1) is not known *a priori*. This was done by assigning a wrong value to the feed flow parameter  $\hat{A}$  in the mathematical model, i.e., for  $\hat{A} \neq A'$ . Unlike the studies discussed in the preceding paragraph, the desired synchronization in the process and the model dynamics could not be achieved for the inaccuracy introduced in the model parameter  $\hat{A}$ . This suggests that the driving conditions [Eqs. (5) and (6)] are not robust enough to bring about synchronization in the present situation and a corrective algorithm for  $\hat{A}$  needs to be introduced.

Mechanisms for parametric self-adaptation have been studied in the context of simpler homogeneous systems [12–15]. In the present case, to formulate a self-adaptation mechanism for an extended system, we begin by introducing a spatial dependence in the feed parameter with  $\hat{A}_{\text{ref}} = \hat{A}(i,0)$ . We then calculate the dynamic adaptation  $\Delta \hat{A}(i,t)$  to be made to the reference value  $\hat{A}_{\text{ref}}$  such that the true process value of  $A'(i,t)$ ,  $i = 1, \dots, N$ , is realized in the mathematical model, i.e.,  $[\hat{A}_{\text{ref}} + \Delta \hat{A}(i,t)] = A'(i,t)$ . For those lattice sites where dynamical process data ( $u'(j,t), v'(j,t)$ ) are available, calculation of the  $\Delta \hat{A}(j,t)$  may be carried out by solving Eqs. (3) and (4) dynamically with a set of  $n_d$  adapter equations, viz.,

$$\begin{aligned} \partial \Delta \hat{A}(j,t) / \partial t = & \epsilon \{ [\hat{u}(j,t) - u'(j,t)] \\ & + [\hat{v}(j,t) - v'(j,t)] \} , \end{aligned} \quad (7)$$

where  $\epsilon$  is a stiffness coefficient for adaptation. Note that for the remaining  $N - n_d$  lattice sites not covered by the adapter equations an average adaptation  $\Delta \hat{A}_{\text{av}}$  in the form  $\sum_j \Delta \hat{A}(j,t) / n_d$  may be implemented. A successful

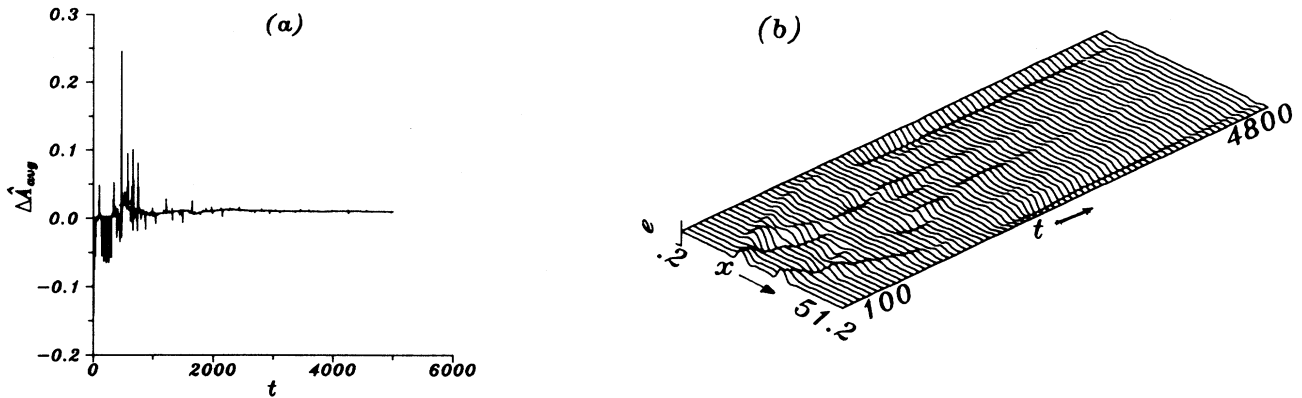


FIG. 2. The synchronization capability of the model [which was initially set in the homogeneous state ( $u = 1, v = 0$ )] and its characterization for inaccurate parameter settings using limited and noisy process data ( $\gamma = 0.0001$ ). (a)  $\Delta \hat{A}_{av}$ , converging to 0.01 for a wrongly set model parameter,  $\hat{A}_{ref} = 0.02$ , when the actual process operating value is  $A'(i, t) = 0.03$ . (b) Progressive decrease in the error function  $e(i, t) = [v(i, t) - \hat{v}(i, t)]$  showing the synchronization between process and model dynamics ( $e$  axis scale:  $-1.63, 0.58$ ).

result for accurate model characterization and its possible synchronization with the process dynamics when  $\hat{A} \neq A'$  is shown in Fig. 2. Note that the above functional form for adaptation is linear and only representative. Other functional forms of adaptation, e.g., cubic, history-linear, sign, etc., are known in the context of controlling simpler systems [14]. Relative assessments in the specific choice of the adapter functional forms and the choice of parameter(s) for adaptation can be made [14]. Further, the choice of  $\epsilon$  may be rationalized by studying the stability characteristics of the combined model and adapter dynamics. As long as the combined system has negative eigenvalues in a linearized region of model phase-space variables, synchronization should be possible. A range of  $\epsilon$  values can satisfy this requirement and moreover, within this range, the magnitude of  $\epsilon$  may indicate the rapidity with which the synchronization occurs [14]. The convergence of  $\Delta \hat{A}_{av}$  to a value 0.01 in Fig. 2(a) (the initial difference in  $A'$  and  $\hat{A}$ ) with dynamic

corrections for noise reduction indicates the accurate estimation of the model parameter. This is also implicit from the diminishing nature of the error function in  $v(x, t)$  [in Fig. 2(b)]. Furthermore, at  $t = 0$ , when the adapter signals were implemented, the response model had initial conditions corresponding to a dormant state, i.e.,  $\hat{u}(i, 0) = 1$  and  $\hat{v}(i, 0) = 0$ , while the process initial condition at this time was assumed to be in the first replicating stage. This indicates the possibility of activating a dormant replicating system and synchronizing its behavior with that of a naturally replicating process even for constraints in the availability of data.

We next turn our attention towards the possible control of the replicating dynamics, in a fashion similar to the above exercise where a model parameter was ascertained by dynamic correction. It may be noted that  $A'$ , being a feed flow parameter, is accessible for external manipulations by an experimenter and can be chosen as a convenient controller variable. We now aim at control-

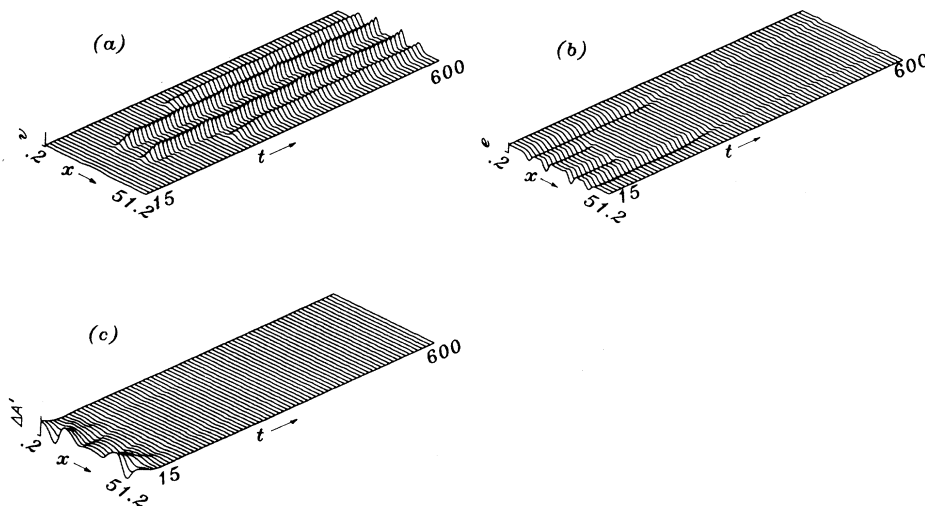


FIG. 3. Control and arrest of replicating growth. (a) Attaining the desired four-peak set-point state ( $u_{set}(i, 800), v_{set}(i, 800)$ ) in Fig. 1, by adaptive control [Eq. (4)] with  $\epsilon = -1.0$  and  $\gamma = 0.0001$ . ( $v$  axis scale:  $-0.17, 1.45$ ). (b) Progressive decrease in the error function  $e(i, t) = [v(i, t) - v_{set}(i, t')]$  while attaining the desired state ( $e$  axis scale:  $-1.45, 0.27$ ). (c) Space-time adaptation signals implemented ( $\Delta A'$  axis scale:  $-1.16, 1.18$ ).

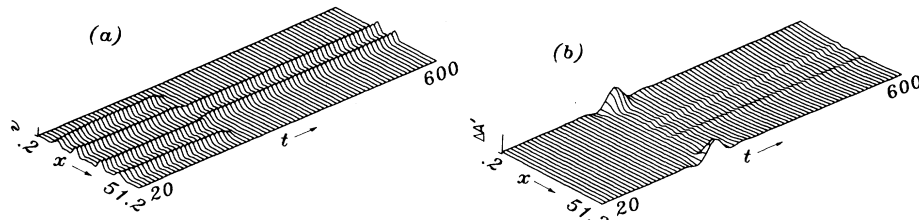


FIG. 4. Bringing a replicating process back in time to a less developed state and arresting the growth in this state. (a) Altering the dynamics from a four-peak replicating stage to a two-peak set-point state, namely,  $(u_{\text{set}}(i, 50), v_{\text{set}}(i, 50))$  in Fig. 1 and future control of the process in this state. Note: The adapter controls were initiated at  $t = 200$ . ( $v$  axis scale:  $-0.16, 1.43$ .) (b) Space-time adaptation signals implemented ( $\Delta A'$  axis scale:  $-0.04, 0.29$ ).

ling the replicating dynamics presented in Fig. 1 with varied and important objectives such as attaining a desired dynamical state, arresting the growth of the pattern in time, negating the effects of noise in the dynamics, etc. For controlling the process we shall now choose to implement on the replicating process itself calculated values of  $A'(i, t)$ , viz.,  $A'(i, t) = A_{\text{ref}} + \Delta A'(i, t)$ , where  $A_{\text{ref}} = A'(i, 0)$ , and  $\Delta A'(i, t)$  may be calculated directly by an appropriate adapter formalism. In this case  $\Delta A'(i, t)$  provides the necessary corrections to the feed flow parameter that need to be implemented such that eventually the desired objectives are realized. We shall exemplify the results for an adapter formalism of the type

$$\partial \Delta A'(i, t) / \partial t = \epsilon [u'(i, t) - u_{\text{set}}(i, t')],$$

$$i = 1, \dots, N, \quad (8)$$

which incorporates data signals in only one system variable, namely,  $u'(i, t)$ , but from every positional site in the spatial domain. We first consider the problem of arresting the replicating process in a desired dynamical state, say the four-peak state specified by  $(u_{\text{set}}(i, 800), v_{\text{set}}(i, 800))$  in Fig. 1. It was assumed that the measurement of  $u'(i, t)$  from the process incorporates noise  $\eta(i, t)$  following a Gaussian distribution (as before). The results presented in Figs. 3(a) and 3(b) suggest that the controlled system effectively attains the desired set-point state [Fig. 3(c)]. Note that the time required to attain the four-peak state is considerably reduced when compared to its natural evolution (i.e., Fig. 1). It may particularly be noted that after realizing the desired set-point state the replicating process dynamics does not propagate further, because, for any deviations of the process dynamics from the set point, corrections via the adapter continuously control the system in the set-point state  $(u_{\text{set}}(i, 800), v_{\text{set}}(i, 800))$ . Allowing the controller mechanism [via Eq. (8)] to be always active in time, i.e., even after the set-point state is attained, ensures that local variations due to noise are continuously negated.

Note that if the controls are switched off, i.e.,  $\Delta A'(i, t) = 0.0$ , the replicating process will begin to propagate from the set-point state following its natural evolution.

It would be interesting to consider the possibility of altering the dynamical state of the system at time, say,  $t$  to that encountered at an earlier time  $t' (< t)$  because inducing an overgrown process to occupy a less developed level is indeed suggestive of system maneuverability by control. A study where an initial four-peak state is seen to rapidly synchronize with the chosen two-peak state and is subsequently pinned for the control mechanism [Eq. (8)] still functioning is shown in Fig. 4(a). Figure 4(b) depicts the corresponding adapter signals to be implemented on the process. Thus the above results (Figs. 3 and 4) suggest that adaptation of an externally manipulable control variable  $A'(i, t)$  allows profitable tuning of the replicating behavior.

The phenomenon of self-replication especially in biological systems [1,7] involves transportation of species and their interactions in a complex and possibly autocatalytic way [16]. The present work analyzes a generic self-replicating model and shows that control may be possible even with limited and inaccurate system information. It may be interesting to note that recent lattice gas cellular automaton simulations of a similar self-replicating mathematical model estimate the order of magnitude of the length and the time scales over which this phenomenon can occur to be considerably within the confines of a eukaryotic cell [5]. Development of experimental techniques to monitor time-series data and implement system controls at these scales is indeed a difficult task. However, it is hoped that with the rapid advances that are taking place in this direction it may become possible to control replicating systems for the aims studied here.

We gratefully acknowledge the support by the Department of Science and Technology, New Delhi, India in carrying out this work.

[1] Y. Kuramoto, *Chemical Oscillations, Waves and Turbulence* (Springer-Verlag, Berlin, 1984); *Oscillations and Travelling Waves in Chemical Systems*, edited by R. J. Field and M. Burger (Wiley, New York, 1985); M. C.

Cross and P. C. Hohenberg, *Rev. Mod. Phys.* **65**, 851 (1993).

[2] V. Castets, E. Dulos, J. Boissonade, and P. De Kepper, *Phys. Rev. Lett.* **64**, 2953 (1990); W. Ouyang and H. L.

- Swinney, *Nature* **352**, 610 (1991).
- [3] K. J. Lee, W. D. McCormick, Q. Ouyang, and H. L. Swinney, *Science* **261**, 192 (1993).
- [4] J. E. Pearson, *Science* **261**, 189 (1993); W. N. Reynolds, J. E. Pearson, and S. Ponce-Dawson, *Phys. Rev. Lett.* **72**, 2797 (1994).
- [5] S. P. Dawson, B. Hasslacher, and J. E. Pearson, in *Pattern Formation and Lattice Gas Automata*, edited by A. Lawniczak and R. Kapral, Fields Institute Communications (American Mathematical Society, Providence, in press).
- [6] K. J. Lee, W. D. McCormick, J. E. Pearson, and H. L. Swinney, *Nature* **369**, 215 (1994).
- [7] A. M. Turing, *Philos. Trans. R. Soc. London Ser. B* **327**, 37 (1952); J. Boissonade, *Nature* **369**, 188 (1994); J. D. Murray, *Mathematical Biology* (Springer, New York, 1989).
- [8] A. P. Bachmann, P. Walde, P. L. Luisi, and J. Lang, *J. Am. Chem. Soc.* **112**, 8200 (1990); **113**, 8204 (1991); A. P. Bachmann, P. L. Luisi, and J. Lang, *Nature* **357**, 57 (1992).
- [9] T. Li and K. C. Nicolaou, *Nature* **369**, 218 (1994); D. Sievers and G. von Kiedrowski, *ibid.* **369**, 221 (1994); C. K. Biebricher, M. Eigen, and W. C. Gardiner, in *Biologically Inspired Physics*, edited by L. Peliti (Plenum, New York, 1991), p. 317.
- [10] P. Gray and S. Scott, *Chem. Eng. Sci.* **38**, 29 (1983).
- [11] L. M. Pecora and T. L. Carroll, *Phys. Rev. A* **44**, 2374 (1991); M. Ding and E. Ott, *Phys. Rev. E* **49**, R945 (1994); W. L. Ditto and L. M. Pecora, *Sci. Am.* **269** (2), 78 (1993).
- [12] B. A. Huberman and E. Lumer, *IEEE Trans. Circuits Syst.* **37**, 547 (1990); S. Sinha and R. Ramaswamy, *Physica D* **43**, 118 (1990).
- [13] V. Ravi Kumar, B. D. Kulkarni, and P. B. Deshpande, *Proc. R. Soc. London Ser. A* **433**, 711 (1991); J. K. Bandyopadhyay, V. Ravi Kumar, B. D. Kulkarni, and P. Bhattacharya, *Chem. Eng. Sci.* **48**, 3545 (1993).
- [14] D. Vassiliadis, *Physica D* **71**, 319 (1994).
- [15] H. K. Qammer, F. Mossayebi, and L. Murphy, *Phys. Lett. A* **178**, 279 (1993); H. D. I. Abarbanel, R. Brown, J. J. Sidorowich, and L. Sh. Tsimring, *Rev. Mod. Phys.* **65**, 1331 (1993).
- [16] H. Meinhardt, in *Biologically Inspired Physics* [9], p. 279.